JOURNAL OF NATURAL PRODUCTS

Article

pubs.acs.org/jnp

HSQC-1,1-ADEQUATE and HSQC-1,*n*-ADEQUATE: Enhanced Methods for Establishing Adjacent and Long-Range $^{13}C-^{13}C$ Connectivity Networks

Gary E. Martin,*[,†] Bruce D. Hilton,[†] and Kirill A. Blinov[‡]

[†]Discovery and Preclinical Sciences, Global Chemistry, Structure Elucidation Group, Merck Research Laboratories, Summit, New Jersey 07901, United States

[‡]Advanced Chemistry Development, Moscow Department, Moscow 117513, Russian Federation

ABSTRACT: $^{1}H-^{13}C$ GHSQC and GHMBC spectra are irrefutably among the most valuable 2D NMR experiments for the establishment of unknown chemical structures. However, the indeterminate nature of the length of the long-range coupling(s) observed via the $^{n}J_{CH}$-optimized delay of the GHMBC experiment can complicate the interpretation of the data when dealing with novel chemical structures. *A priori* there is no way to differentiate $^{2}J_{CH}$ from $^{n}J_{CH}$ correlations, where $n \geq 3$. Access to high-field spectrometers with cryogenic NMR probes brings 1,1- and 1,*n*-ADEQUATE experiments into range for modest samples. Subjecting ADEQUATE spectra to covariance processing with high sensitivity experiments such as multiplicity-edited GHSQC affords a diagonally symmetric $^{13}C-^{13}C$ correlation spectrum in which correlation data are observed with the apparent sensitivity of the GHSQC spectrum. HSQC-1,1-ADEQUATE covariance spectra derived by co-processing of GHSQC and 1,1-ADEQUATE spectra allow the carbon skeleton of molecules to be conveniently traced. HSQC-1,*n*-ADEQUATE spectra provide enhanced access to correlations equivalent to $^{4}J_{CH}$ correlations in a GHMBC spectrum. When these data are used to supplement GHMBC data, a powerfully synergistic set of heteronuclear correlations are available. The methods discussed are illustrated using retrorsine (**1**) as a model compound.

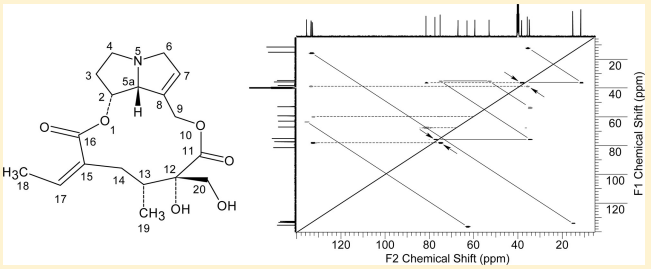

Two-dimensional NMR methods have revolutionized the elucidation of complex chemical and natural product structures. Heteronuclear shift correlation methods can be considered as one of the cornerstones of modern structure elucidation protocols. Higher field spectrometers coupled with modern cryogenic NMR probes have made it possible to acquire direct and long-range heteronuclear shift correlation spectra in reasonable periods of time on submicromole samples.[1] When samples in the range of ~1 mg of material are available, 1,1- and 1,*n*-ADEQUATE[2−5] are feasible as overnight or weekend acquisitions, respectively, on instruments equipped with a 1.7 mm MicroCryoProbe.[1,6,7] Recently, it has been shown that subjecting ADEQUATE spectra to unsymmetrical indirect (UIC)[8] or generalized indirect covariance (GIC)[9] processing with a high-sensitivity experiment such as multiplicity-edited GHSQC spectra can provide access to carbon−carbon ADEQUATE connectivity information with the much higher inherent sensitivity of the GHSQC spectrum.[6,7,10−12] Moreover, the carbon−carbon connectivity information is displayed in a "COSY-like", diagonally symmetric spectrum that incorporates the multiplicity editing of the GHSQC spectrum used in the calculation. The calculation and interpretation of HSQC-1,1-ADEQUATE and HSQC-1,*n*-ADEQUATE spectra of the alkaloid retrorsine (**1**) are used to illustrate the method. The issue of modulation of correlations of adjacent responses in 1,1-ADEQUATE spectra is also considered.

1

RESULTS AND DISCUSSION

Long-range $^{1}H-^{13}C$ heteronuclear couplings observed in GHMBC spectra predominantly arise from $^{3}J_{CH}$ coupling pathways, although, *a priori*, there is no way to differentiate among the $^{n}J_{CH}$ coupling pathways that are possible where n = 2−4. Long-range heteronuclear shift correlation methods have been reviewed.[13] The indeterminate nature of the length of a given long-range correlation in GHMBC spectra led to the development of the $^{2}J^{3}J$-GHMBC experiment,[14] which was subsequently followed by the development of the H2BC[15,16] and HAT-H2BC[17] experiments. These experiments are capable

Received: June 22, 2011
Published: November 4, 2011

of identifying adjacent protonated carbons, but cannot identify nonprotonated, adjacent carbon resonances. In contrast, 1,1-ADEQUATE[2−4] spectra can identify adjacent, nonprotonated neighbor carbon resonances albeit with considerably lower sensitivity than variants of the GHMBC experiment.[14−17] Unfortunately the 1,1-ADEQUATE experiment cannot identify adjacent nonprotonated carbon pairs. It is likely that the inherently low sensitivity of the ADEQUATE-type experiments has contributed to the dearth of applications in the literature, which has been recently reviewed.[18] Finally, the INADEQUATE experiment, which is elegantly capable of mapping out the full carbon skeleton of a molecule with the only gaps due $^{13}C-^{13}C$ AB resonance pairs, is far less sensitive than the 1,1-ADEQUATE experiment with prodigious sample requirements.[19−21]

Covariance NMR methods have also been the subject of a recent review.[22] Perhaps the most powerful application of these methods yet to be described is the ability to mathematically combine pairs of experiments that share a common frequency domain using either UIC[8] or GIC[9] co-processing. This capability provided the basis for the recent reports detailing the combination of multiplicity-edited GHSQC and 1,1-ADEQUATE spectra.[6,7,10,11,23]

There are several attributes of covariance-calculated spectra such as HSQC-1,1-ADEQUATE and HSQC-1,*n*-ADEQUATE that make them quite attractive for use in structure elucidation protocols. First, as with other UIC[8]- or GIC[9]-calculated hyphenated 2D NMR spectra, the 1,1-ADEQUATE-derived adjacent carbon−carbon correlations are observed with the apparent intrinsic sensitivity of the multiplicity-edited GHSQC experiment rather than the much lower sensitivity of the 1,1-ADEQUATE spectrum itself.[6,10] Second, the phase-encoded multiplicity editing of the GHSQC experiment is retained in the hyphenated spectrum. Third, carbon−carbon correlations between adjacent protonated carbon pairs are observed in a diagonally symmetric spectrum that is analogous to the familiar COSY spectrum. Finally, correlations between adjacent protonated and nonprotonated neighbor carbons are observed at the F_2 shift of the nonprotonated resonance and the F_1 shift of the protonated resonance.[23] These responses are diagonally asymmetric. This latter group of correlations are not observed in $^2J^3J$-GHMBC[14] or H2BC spectra.[15−17] Hence, except for gaps between adjacent nonprotonated carbons and those due to annular heteroatoms, the carbon skeleton of a molecule such as strychnine can be conveniently traced using an HSQC-1,1-ADEQUATE spectrum.[6] Using HSQC-1,1-ADEQUATE spectra, correlations between overlapped resonances in the spectra of the triazolone antifungal agent posaconazole[7] and the CDK-2 inhibitor dinaciclib[11] could also be conveniently traced out.

1,1-ADEQUATE of Retrorsine. The 60 Hz optimized 1,1-ADEQUATE spectrum of retrorsine, **1**, is shown in Figure 1 overlaid with the multiplicity-edited GHSQC spectrum. The 60 Hz optimization for the 1,1-ADEQUATE spectrum was chosen on the basis of the recent report of Cheatham and co-workers,[24] who observed that correlations between adjacent sp^3 carbons are observed with reasonable intensity with a 60 Hz optimization of the $^1J_{CC}$ delay in the pulse sequence for the carbon−carbon couplings. Cheatham et al.[24] also noted that correlations involving sp^2 carbons may be missed when the 1,1-ADEQUATE experiment is, for example, optimized for a 40 Hz $^1J_{CC}$ coupling.

Fundamentally, there are two ways to extract carbon−carbon connectivities from the ADEQUATE data. Correlations can be extracted from either "rows" or "columns" in the 1,1-ADEQUATE spectrum.[18] An example of each approach to extracting the carbon−carbon connectivity information is shown in Figure 1. The network of carbon−carbon connectivities that were extracted from the 60 Hz optimized 1,1-ADEQUATE spectrum of retrorsine, **1**, is shown superimposed on the structure in Figure 2. All of the expected correlations between protonated carbons and their adjacent carbon neighbors are observed in the 60 Hz optimized 1,1-ADEQUATE spectrum with the exception of the correlation between the C-17 methine sp^2 carbon and the adjacent C-15 nonprotonated sp^2 neighbor.

On the basis of the absence of the C-17→C-15 correlation in the 60 Hz 1,1-ADEQUATE spectrum, a second spectrum was acquired overnight optimized for 40 Hz. It was interesting to note that a prominent response was observed in the 40 Hz optimized spectrum at the proton shift of the H-17 methine proton resonating at 5.69 ppm for the correlation to the C-15

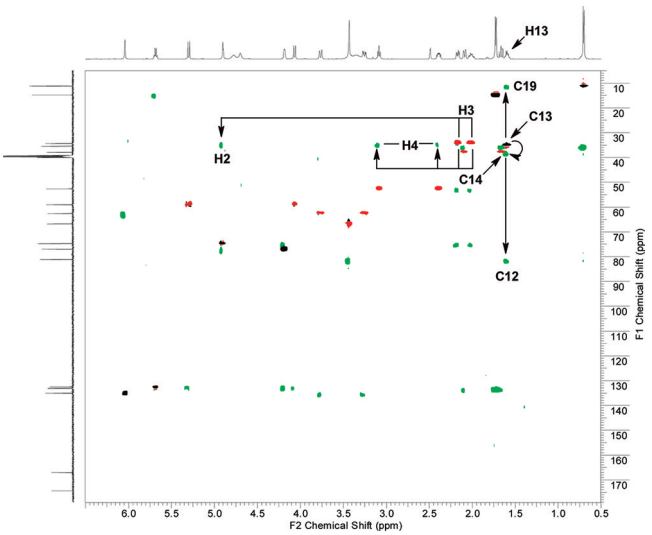

Figure 1. Overlaid multiplicity-edited GHSQC and 60 Hz optimized 1,1-ADEQUATE spectra of a 1.6 mg sample of retrorsine (**1**) dissolved in 30 μL of DMSO-d_6. The 1,1-ADEQUATE data were acquired in 18 h 23 min. The correlations from the multiplicity-edited GHSQC spectrum are plotted in black for the positively phased responses for the methine and methyl resonances and in red for the inverted responses for the methylene resonances. Correlations from the 1,1-ADEQUATE spectrum are plotted in green. Correlation information can be extracted from the 1,1-ADEQUATE data using either columns or rows in the spectrum. Using the H-13/C-13 methine pair to illustrate a column, the direct correlation is observed at 1.60/35.4 ppm ($^1H/^{13}C$). Correlations are observed in the column defined the by ^1H shift of C-13 (1.60 ppm) at 11.5 ppm (C-19 methyl), 37.9 ppm (C-14 methylene), and 81.1 ppm (C-12 quaternary). These correlations establish the identities of the three adjacent carbon resonances centered at C-13. As an example of extracting information from a row, the anisochronous H-3 methylene protons resonating at 2.17 and 2.02 ppm are used as an example. The horizontal connectivity arrows from the 2.17, 2.02/34.4 ppm ($^1H/^{13}C$) show the correlations at the proton shifts of the adjacent H4-methylene protons resonating at 3.08 and 2.39 ppm. The correlations arise from the carbon−carbon connectivity between the C-4 methylene resonating at 52.6 ppm and the H-3 methylene carbon resonating at 34.4 ppm. A correlation is also observed at 4.91 ppm, the chemical shift of the H-2 methine resonance. The correlation arises from the carbon−carbon connectivity between the C-2 methine carbon resonating at 74.8 ppm and the C-3 methylene resonance at 34.4 ppm.

dx.doi.org/10.1021/np200540q | *J. Nat. Prod.* 2011, 74, 2400−2407

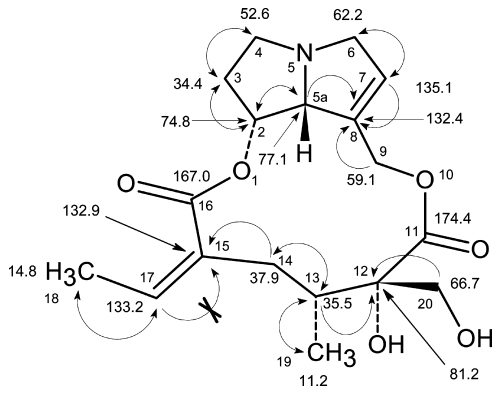

Figure 2. Carbon−carbon connectivities extracted from the 60 Hz optimized 1,1-ADEQUATE spectrum shown in Figure 1 accompanied by assigned ^{13}C shifts. All of the expected correlations between protonated carbon pairs and protonated carbons and adjacent nonprotonated neighbor carbons were observed with the exception of the correlation from C-17 to C-15. Double-headed arrows denote mutually correlated protonated carbon resonant pairs; single-headed arrows denote correlations from protonated to nonprotonated adjacent carbon resonances.

nonprotonated carbon resonating at 132.9 ppm. This observation was contrary to the work of Cheatham and co-workers,[24] which suggested that the opposite should be true. To probe the issue of the modulation of the C-17→C-15 correlation as a function of the optimization of the $^1J_{CC}$ coupling delay, a series of 1,1-ADEQUATE spectra optimized in 5 Hz steps were acquired. Segments of five of these spectra, optimized at 30, 35, 40, 45, and 60 Hz, are plotted in Figure 3. As is clearly shown, a prominent response (boxed region) is observed for the C-17→C-15 correlation in the 30 Hz spectrum that becomes progressively weaker in the 35 and 40 Hz spectra before disappearing completely in the 45 and 60 Hz optimized spectra. A trend is observed for the correlation between the C-9 methylene and C-8 quaternary sp^2 carbons, although in the opposite direction. A strong correlation is observed in the spectra optimized for 40−60 Hz (dashed boxed) that becomes weak in the 35 Hz optimized spectrum and is lost completely in the 30 Hz optimized experiment. As confirmed by the data shown in Figure 3, the optimization of the $^1J_{CC}$-based delay in 1,1-ADEQUATE spectra can sometimes be problematic. Similar problems in the elucidation of the structure of a marine natural product, jamaicamide, prompted Williamson and co-workers[26] to report the development of the ACCORD-ADEQUATE experiment in which the $^1J_{CC}$-based delays are accordion-optimized. We are investigating the development of a version of the ACCORD-ADEQUATE experiment that incorporates CHIRP pulses[4] to both improve sensitivity and diminish the likelihood of losing responses due to optimization choices; this work will be the topic of a future report.

HSQC-1,1-ADEQUATE of Retrorsine. Unsymmetrical indirect[8] or generalized indirect covariance[9] processing of 2D NMR experiments that share a common frequency domain provides high-sensitivity access to the correlation information contained in hyphenated 2D NMR spectra that often have considerably lower relative sensitivity than the component spectra or the low-sensitivity member of the co-processed pair of spectra.[6,10,26,27]

Subjecting a pair of 2D NMR spectra that share a common frequency domain to UIC[8] processing affords an asymmetric covariance spectrum. In contrast, the GIC processing method

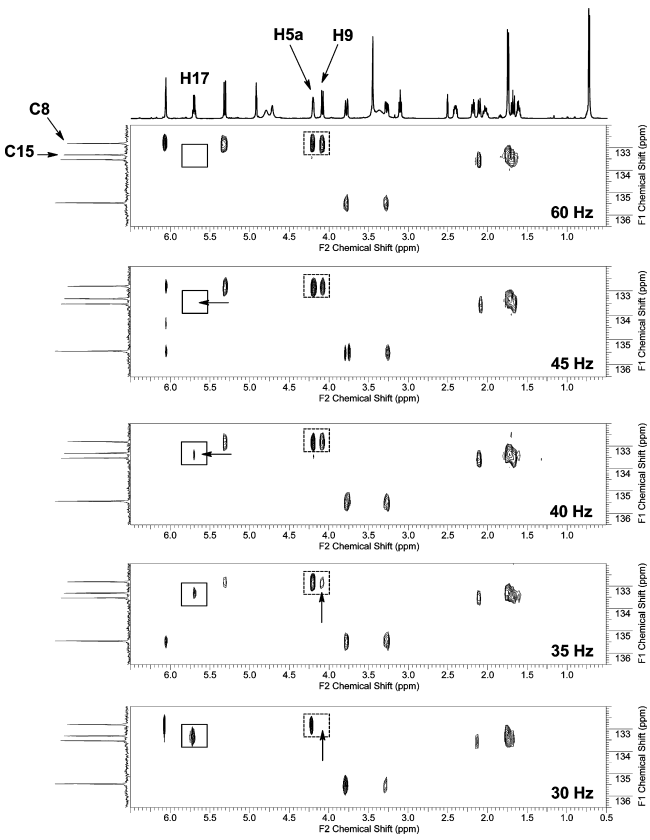

Figure 3. Segments of the sp^2 carbon region of a series of 1,1-ADEQUATE spectra of retrorsine (**1**) in which the $^1J_{CC}$ coupling was optimized over the range from 30 to 60 Hz. In the 30 and 35 Hz spectra, the C-17→C-15 $^1J_{CC}$ correlation (solid boxes) is observed with good intensity. In the 40 Hz spectrum, the intensity of this correlation has decreased significantly, and in the 45 and 60 Hz spectra, the response is completely absent. A modulation is also observed for the C-9→C-8 correlation (dashed boxes). In the 60, 45, and 40 Hz spectra, this correlation is observed with good intensity. In the 35 Hz spectrum, the C-9→C-8 has become weak, and in the 30 Hz spectrum it is completely absent. All of the spectral segments were plotted using the same threshold.

affords a symmetric spectrum that is amenable to matrix root processing operations, e.g., square root calculations, which can reduce artifact intensity and noise in some cases.[9]

Recently, we reported that 1,1-ADEQUATE spectra can also be subjected to either UIC or GIC co-processing with multiplicity-edited GHSQC spectra to afford HSQC-1,1-ADEQUATE spectra in which the adjacent carbon−carbon connectivity information is observed with the apparent, higher intrinsic sensitivity of the GHSQC experiment.[6,7,10,11] Using the 60 Hz optimized 1,1-ADEQUATE spectrum of retrorsine (**1**) shown in Figure 1, the HSQC-1,1-ADEQUATE covariance spectrum shown in Figure 4 was calculated using the generalized indirect covariance processing method of Snyder and Brüschweiler[9] with power = 0.5. The information content of the spectrum is identical to that of the 1,1-ADEQUATE spectrum with the exception that correlations are observed with better S/N as a result of the covariance calculation[11] and problems inherent to proton resonance overlaps are often circumvented by the inherently higher dispersion of the carbon−carbon correlations of HSQC-1,1-ADEQUATE spectra.[7] The HSQC-1,1-ADEQUATE covariance spectrum shown in Figure 4 is diagonally symmetric for correlations between

dx.doi.org/10.1021/np200540q | J. Nat. Prod. 2011, 74, 2400−2407

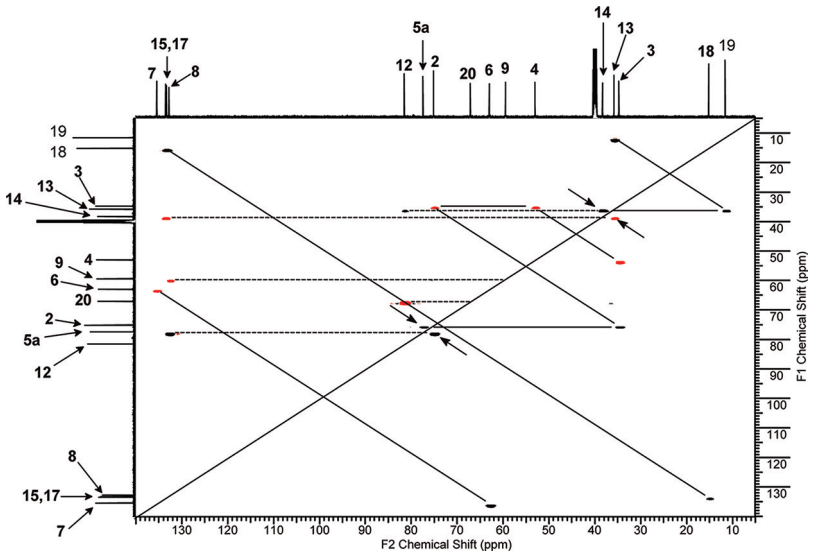

Figure 4. HSQC-1,1-ADEQUATE spectrum of retrorsine (**1**) calculated using the GIC method (power = 0.5) from the 60 Hz optimized 1,1-ADEQUATE spectrum shown in Figure 1 and the multiplicity-edited GHSQC spectrum that was overlaid in Figure 1. Response information in the spectrum is phase-encoded based on the multiplicity editing of the GHSQC spectrum used in the calculation. Methine and methyl resonances (F_1) have positive phase and are plotted in black; methylene resonances (F_1) are negatively phased and are plotted in red. The spectrum is diagonally symmetric for adjacent protonated carbon resonant pairs. Correlations between protonated and nonprotonated adjacent carbons are observed at the F_2 shift of the nonprotonated carbon resonance and the F_1 shift of the protonated carbon. The responses are observed with the phase of the protonated carbon resonance. As an example, beginning with the correlation for the 19-methyl resonance (11.2 ppm), the correlation to the adjacent C-13 methine resonance (35.5 ppm) is designated by the solid line perpendicular to the diagonal in Figure 4. The solid horizontal line at the F_1 shift of C-13 next identifies the adjacent C-14 methylene resonance (37.9 ppm, diagonal symmetry) and the C-19 methyl resonance. The dashed horizontal line beyond the C-14 correlation identifies the correlation from C-13 to the C-12 quaternary carbon (81.1 ppm). The C-14 methylene resonance is, in turn, finally correlated via the dashed horizontal line to the C-15 nonprotonated methine carbon (132.9 ppm).

adjacent protonated carbons and retains the phase-encoded multiplicity information of the GHSQC spectrum. Correlations between adjacent protonated carbons are designated by solid lines perpendicular to the diagonal. Horizontal solid lines are used to designate connectivities of a given protonated carbon to protonated adjacent carbon neighbors. Dashed horizontal lines indicate correlations from a protonated carbon to an adjacent nonprotonated carbon neighbor.

Starting from any arbitrary point in the HSQC-1,1-ADEQUATE covariance spectrum, the carbon−carbon connectivity network can be traced for the segment of the molecular structure containing the response selected as a starting point. Generally, the only interruptions to the connectivity network are those due to heteroatoms and consecutive nonprotonated carbons; the latter are not correlated to each other in a 1,1-ADEQUATE spectrum.

A comparison of the sensitivity advantage garnered from covariance processing of the data is shown in Figure 5. Using the region from 95 to 100 ppm, which is devoid of responses in the ^{13}C spectrum of **1**, to define noise, the S/N ratio for the C-5a methine resonance (77.1 ppm) in the 60 Hz optimized 1,1-ADEQUATE spectrum (Figure 1) was 89:1 (see Figure 5B). In contrast, for the same resonance in the HSQC-1,1-ADEQUATE covariance spectrum shown in Figure 4, the S/N ratio was 536:1 (see Figure 5C). Covariance processing sensitivity gains range from the ~6-fold increase in this study to as much as 20-fold in other cases.[6,10] Using covariance processing methods, it is feasible to either decrease the data acquisition time for the 1,1-ADEQUATE spectrum or conversely to reduce the size of the sample used to acquire the data.[10]

1,*n*-ADEQUATE of Retrorsine. The 1,1-ADEQUATE and covariance calculated HSQC-1,1-ADEQUATE spectra rely on the relatively large $^1J_{CC}$ coupling constant for the carbon−carbon out-and-back magnetization transfer. In the initial reports of Köck and co-workers,[2−4] several other ADEQUATE variants were described that included 1,*n*-, *n*,1-, and *n*,*n*-ADEQUATE.[18] These variants differ from 1,1-ADEQUATE in the optimization of the various delays in the pulse sequence. In the case of the 1,1-ADEQUATE experiment, the 1,1-prefix designates the $^1J_{CH}$ and $^1J_{CC}$ couplings, respectively, via which magnetization transfers occur in the experiment. In the case of the 1,*n*-ADEQUATE experiment transfers are via $^1J_{CH}$ and $^nJ_{CC}$ couplings, respectively. The reader interested in the *n*,1-ADEQUATE and *n*,*n*-ADEQUATE variants is referred to a recent review by Martin.[18]

There have been only a few reported applications of the 1,*n*-ADEQUATE experiment.[2,3,5,12] In part, the lack of applications can be largely attributed to the approximately 4-fold lower sensitivity of the 1,*n*-ADEQUATE experiment vs the 1,1-ADEQUATE experiment. However, when one considers the magnetization transfers involved, i.e., $^1J_{CH}$ followed by $^nJ_{CC}$, typically using an optimization of ~5−11 Hz, correlations are observed that are the equivalent of $^3J_{CH}$ or $^4J_{CH}$ long-range correlations in a GHMBC spectrum.[2−6,12] If one considers the correlation data that can be derived from 1,1-ADEQUATE, GHMBC, and 1,*n*-ADEQUATE spectra in sequence, the correlations are the equivalent to exclusively $^2J_{CH}$, primarily $^3J_{CH}$, and a mix of $^3J_{CH}$ and $^4J_{CH}$ correlations, respectively, in a hierarchical manner. These correlation data are a powerful adjunct in the elucidation of novel chemical structures of any type, resorting only to those experiments necessary to solve a given problem. Furthermore, these data can also provide useful input for computer-assisted structure elucidation (CASE) programs.[5,24]

dx.doi.org/10.1021/np200540q | *J. Nat. Prod.* 2011, 74, 2400−2407

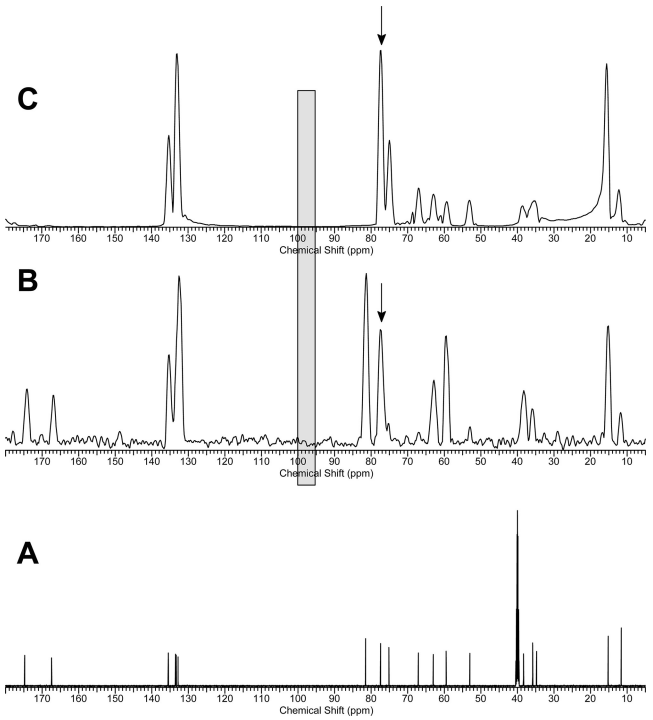

Figure 5. (A) High-resolution ^{13}C reference spectrum of a 1.6 mg sample of retrorsine (**1**) in 30 μL of DMSO-d_6. (B) F_1 projection of the 60 Hz optimized 1,1-ADEQUATE spectrum of the sample of retrorsine recorded in 18 h 30 min. (C) Positive F_1 projection of the 60 Hz HSQC-1,1-ADEQUATE covariance spectrum of the same sample calculated from the 60 Hz 1,1-ADEQUATE spectrum shown in Figure 1 and a multiplicity-edited GHSQC spectrum recorded in 8 min. The grayed region from 95 to 100 ppm was arbitrarily chosen as representative noise. Using the C-5a methine resonance at 77.1 ppm (designated by the arrow) as a comparator, the S/N ratio of the 1,1-ADEQUATE spectrum was 89:1. In contrast, the S/N for the same resonance in the HSQC-1,1-ADEQUATE covariance spectrum was 536:1. Typical sensitivity gains arising from covariance processing have ranged from the factor of ~6-fold observed in this comparison to as much as 20-fold.[6,10]

Investigator access to high-field NMR instruments equipped with cryogenic probes, coupled with the sensitivity gains inherent to covariance-calculated NMR spectra, should increase interest in the use of 1,1-ADEQUATE and 1,*n*-ADEQUATE experiments in structure elucidation protocols. It was on this basis that the 1,*n*-ADEQUATE spectra of retrorsine (**1**) were investigated.

The 1,*n*-ADEQUATE spectrum of **1** optimized for 7 Hz for the $^nJ_{CC}$ couplings is shown in Figure 6. The disposition of data in the spectrum is analogous to the 1,1-ADEQUATE spectrum shown in Figure 1 and can be interpreted in the same manner (see Figure 6). Correlations are observed at the F_2 frequency of the direct proton−carbon pair from which the correlation process began via $^1J_{CH}$ and at the F_1 frequency of the carbon to which the directly bound carbon is long-range coupled via $^nJ_{CC}$. The spectrum shown in Figure 6 contains a mix of $^1J_{CC}$ and $^nJ_{CC}$ correlations; no effort was made to suppress the former since the data shown in Figure 1 were available to identify adjacent carbon correlations. The $^nJ_{CC}$ correlations observed for retrorsine (**1**) are a mix of $^2J_{CC}$ and $^3J_{CC}$ correlations (equivalent to $^3J_{CH}$ and $^4J_{CH}$ correlations in a GHMBC spectrum). In contrast, in the process of characterizing a series of mono- and dibromo phakellin and isophakellin alkaloids, Myer and Köck[5] reported only the observed $^3J_{CC}$ correlations, with no mention made of any $^2J_{CC}$ correlations. Unfortunately, the optimization conditions used by the authors were not reported. Experience with strychnine has shown that carbons adjacent to sp^2 carbons as well as annular oxygen and nitrogen atoms are prone to exhibit $^2J_{CC}$ correlations, while carbons flanked by other aliphatic carbons tend to exhibit only $^3J_{CC}$ correlations.[12,18,28] The ensemble of observed $^nJ_{CC}$ correlations for retrorsine (**1**) is summarized in Figure 7.

HSQC-1,*n*-ADEQUATE. In a manner analogous to the calculation of the HSQC-1,1-ADEQUATE covariance spectrum discussed above, 1,*n*-ADEQUATE spectra are also amenable to the UIC[8] or GIC[9] calculation of the corresponding HSQC-1,*n*-ADEQUATE covariance spectrum that is shown in Figure 8. Again, the spectrum is diagonally symmetric, although the correlated protonated carbon resonances are primarily correlated via $^nJ_{CC}$. Some correlations are, however, observed via $^1J_{CC}$ couplings, which are analogous to the incompletely canceled residual direct responses sometimes observed in GHMBC spectra. Long-range correlations between protonated and nonprotonated carbons are again diagonally asymmetric. Correlations to nonprotonated carbons are observed at the F_2 frequency of the nonprotonated carbon and the F_1 frequency of the protonated carbon in the spectrum as shown and labeled in Figure 8.

Long-range coupled protonated carbon pairs are denoted on the spectrum shown in Figure 8 by solid lines perpendicular to the diagonal. Correlations to nonprotonated carbons are designated by dashed horizontal lines. The diagonal symmetry of the HSQC-1,*n*-ADEQUATE spectrum allows the identification of correlations in cases when the responses for one of the $^nJ_{CC}$ coupled resonances may be weak. Intense, negatively phased correlations (red) are observed at the C-20 F_1 shift (66.7 ppm) and the F_2 shifts of the C-13 (35.5 ppm) and C-14 (37.9 ppm) resonances. The corresponding, diagonally symmetric responses at the F_1 shifts of C-13 and C14 along the vertical axis defined by the chemical shift of C-20 were not observed in the spectrum at the threshold plotted. However, by simply going deeper into the data matrix (see inset in Figure 8), the requisite correlations with the proper phase characteristics were observed. A weaker correlation, identified in the same manner, is observed at the ^{13}C shift of the C-19 methyl group. The corresponding response along the vertical axis defined by C-20 was much weaker than those for C-13 and C-14 shown in the inset in Figure 8.

F_1 projections of the 7 Hz optimized 1,*n*-ADEQUATE and the HSQC-1,*n*-ADEQUATE covariance spectrum calculated from the spectrum shown in Figure 8 are compared in Figure 9. The region from 95 to 100 ppm was again used to define noise, and the C-5a methine resonance was again used as a comparator. The S/N ratio for the 7 Hz 1,*n*-ADEQUATE spectrum was measured as 29:1. Using the same resonance from the F_1 projection of the 7 Hz optimized HSQC-1,*n*-ADEQUATE covariance spectrum, the S/N ratio was 436:1, which corresponds to a 16-fold enhancement.

The 1,1- and 1,*n*-ADEQUATE experiments provide the means of establishing the identity of adjacent carbons via $^1J_{CC}$ and long-range coupled carbons via $^nJ_{CC}$ coupling pathways, respectively. The former data have been shown to be highly useful as input data for computer-assisted structure elucidation.[5,24] In cases where $^3J_{CC}$ correlation responses can be differentiated from $^2J_{CC}$ responses, 1,*n*-ADEQUATE data should also have considerable utility. We have shown in the

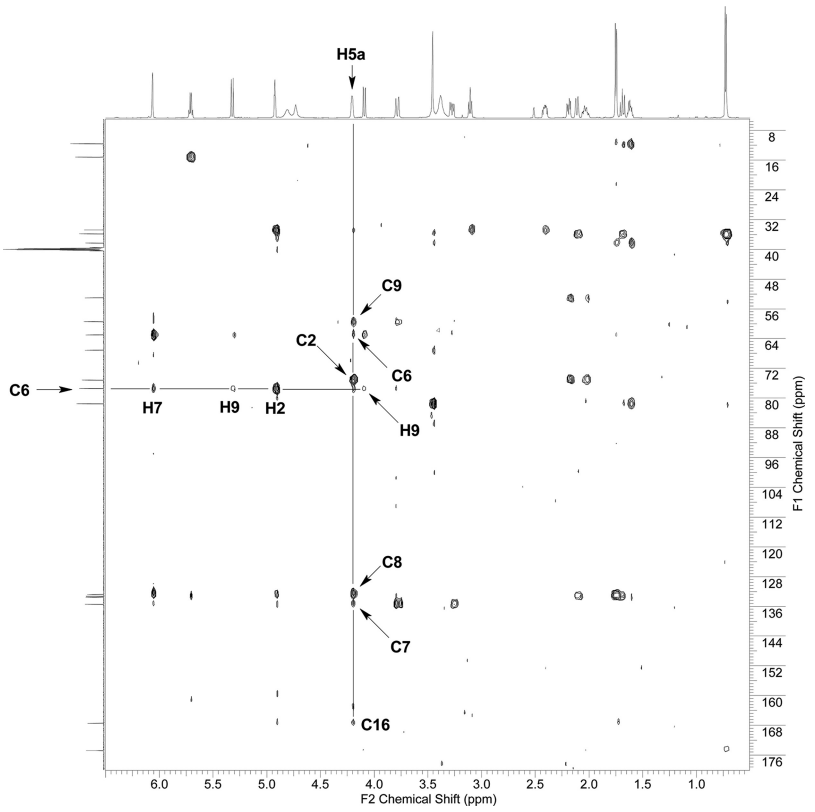

Figure 6. 1,*n*-ADEQUATE spectrum of retrorsine (**1**) optimized for a 7 Hz $^{n}J_{CC}$ coupling; the data were acquired in 18 h 50 min. The 1,*n*-ADEQUATE spectrum can be interpreted via either rows or columns. Correlations labeled along the row defined by the ^{13}C shift of C6 illustrate the former. Correlations are observed via $^{3}J_{CC}$ from C-2 and C-9 at the proton shifts of H-2 and H-9, respectively. The correlation from H-7 is a $^{1}J_{CC}$ correlation that no effort was made to suppress. Interpretation along a column is illustrated for the H-5a resonance. Correlations are observed from the C-5a resonance via $^{2}J_{CC}$ to C-6, C-7, and C-9. A $^{3}J_{CC}$ correlation is observed to the C-16 carbonyl, and residual $^{1}J_{CC}$ correlations are observed to C-2 and C-8.

present study that 1,1- and 1,*n*-ADEQUATE data can be subjected to covariance processing with a corresponding significant improvement in S/N ratios, allowing carbon−carbon connectivity data to be observed with the higher relative sensitivity of the multiplicity-edited GHSQC spectrum with which the ADEQUATE data are co-processed. The sensitivity enhancement that arises from the covariance processing should afford investigators greater experimental access to adjacent and long-range ADEQUATE $^{13}C-^{13}C$ correlation data through a combination of reduced experiment times and/or reduced sample sizes.[10]

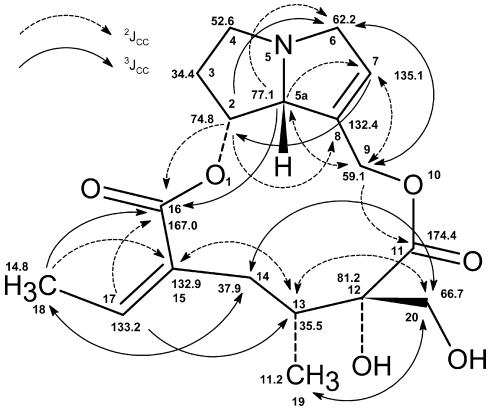

Figure 7. Complete analysis of the carbon−carbon long-range couplings observed in the 7 Hz optimized 1,*n*-ADEQUATE spectrum of retrorsine shown in Figure 6. The observed long-range carbon−carbon correlations consisted of a mix of $^{2}J_{CC}$ and $^{3}J_{CC}$ correlations (corresponding to $^{3}J_{CH}$ and $^{4}J_{CH}$ correlations in a GHMBC spectrum, respectively). Double-headed arrows denote mutually long-range coupled pairs of carbon resonances. $^{1}J_{CC}$ correlations observed in the 1,*n*-ADEQUATE spectrum are not shown.

EXPERIMENTAL SECTION

General Experimental Procedures. All NMR data reported in this study were acquired using a sample of 1.6 mg of retrorsine (Aldrich) dissolved in 30 μL of 99.96% DMSO-d_6 (Cambridge Isotope Laboratories) that was transferred to a 1.7 mm NMR tube (Bruker) using a 24G flexible Teflon needle attached to a Hamilton gastight syringe. All of the NMR data were acquired using a 600 MHz Bruker three-channel AVANCE III NMR spectrometer equipped with a Bruker 1.7 mm TCI $^{1}H/^{13}C-^{15}N$ gradient triple resonance MicroCryoProbe. Data were accumulated with the sample temperature maintained at 30 °C. The GHSQC spectrum was acquired as a 2048 × 512 matrix (ns = 4; acquisition time 55 min); the 1,1-ADEQUATE data were acquired as a 2048 × 160 matrix optimized for 60 Hz (ns = 128; acquisition time 18 h 22 min) spectra; the 1,*n*-ADEQUATE data were acquired as a 2048 × 128 matrix optimized for 7 Hz (ns = 512, acquisition time 60 h 46 min). No effort was made to suppress $^{1}J_{CC}$ correlations in the 1,*n*-ADEQUATE spectrum. The 1,1-ADEQUATE pulse sequence (adeq11etgprdsp) from the Bruker pulse sequence library was used to acquire both the 1,1- and 1,*n*-ADEQUATE data without any modification other than delay duration. The series of 1,1-ADEQUATE spectral segments shown in Figure 3 were taken from 2048 × 160 point spectra with the delay for the $^{1}J_{CC}$ coupling varied in 5 Hz steps over the range from 30 to 65 Hz. The series

dx.doi.org/10.1021/np200540q | *J. Nat. Prod.* 2011, 74, 2400−2407

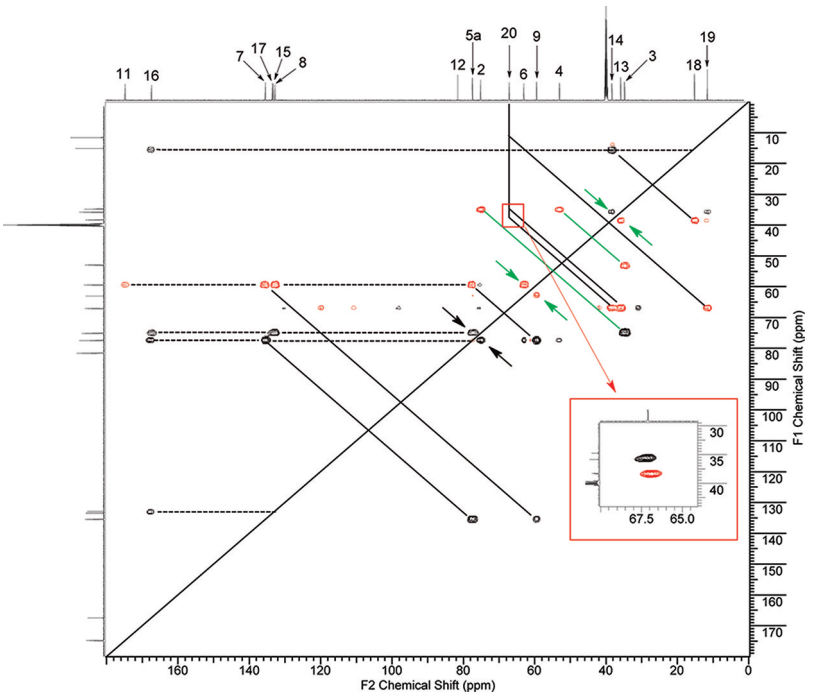

Figure 8. HSQC-1,*n*-ADEQUATE spectrum calculated from the 7 Hz optimized 1,*n*-ADEQUATE spectrum shown in Figure 6 and the multiplicity-edited GHSQC spectrum acquired on the same sample. The spectrum is diagonally symmetric, as is the HSQC-1,1-ADEQUATE spectrum shown in Figure 4. Long-range coupled quaternary carbons are observed at the F_2 frequency of the quaternary carbon and the F_1 frequency of the protonated carbon to which it is coupled. Correlations from the C-20 resonance at the C-20 chemical shift (66.7 ppm) are below the threshold used to prepare the plot shown. The inset shows the diagonally symmetric correlations to the C-13 and C-14 methine and methylene correlations. In a similar manner, a correlation is also observed from the 19-methyl resonance to C-20 that is below the threshold of the contour plot (not shown). Nevertheless, correlations can be identified by virtue of the diagonal symmetry of the spectrum, allowing weaker counterparts to be readily identified, thereby confirming the correlation. Residual $^1J_{CC}$ correlations between adjacent carbons are denoted by green lines perpendicular to the diagonal or green arrows.

of spectra were all acquired using ns = 128, which gave acquisition times ranging from 18 h 20 min to 18 h 30 min. The GHSQC data were zero-filled prior to the second Fourier transform to afford a final 1K × 1K spectrum; the 1,1- and 1,*n*-ADEQUATE data were linear predicted to 512 points in F_1 and then zero-filled to afford a final 1K × 1K spectra. Covariance spectra were calculated using either the unsymmetrical indirect covariance method of Martin et al.[8] or the generalized indirect covariance method of Snyder and Brüschweiler[9] (power = 0.5).

AUTHOR INFORMATION

Corresponding Author

*Phone: +908.473.5398. Fax: +908.473.6559. E-mail: gary.martin2@merck.com.

REFERENCES

(1) Hilton, B. D.; Martin, G. E. *J. Nat. Prod.* **2010**, *73*, 1465−1469.
(2) Köck, M.; Rief, B.; Fenical, W.; Griesinger, C. *Tetrahedron Lett.* **1996**, *37*, 363−366.
(3) Rief, B.; Köck, M.; Kerssebaum, R.; Kang, H.; Fenical, W.; Griesinger, C. *J. Magn. Reson.* **1996**, *118A*, 282−285.
(4) Köck, M.; Kerssebaum, R.; W. Bermel, W. *Magn. Reson. Chem.* **2003**, *41*, 65−69.
(5) Myer, S. W.; Köck, M. *J. Nat. Prod.* **2008**, *71*, 1524−1529.
(6) Martin, G. E.; Hilton, B. D.; Blinov, K. A. *Magn. Reson. Chem.* **2011**, *49*, 248−252.
(7) Martin, G. E. *J. Heterocycl. Chem.*, **2011**, *48*, in press.
(8) Blinov, K. A.; Larin, N. I.; Williams, A. J.; Zell, M.; Martin, G. E. *Magn. Reson. Chem.* **2006**, *44*, 107−109.
(9) Snyder, D. A.; Brüschweiler, R. *J. Chem. Phys. A* **2009**, *113*, 12898−12902.
(10) Martin, G. E.; Hilton, B. D.; Willcott, M. R. III; Blinov, K. A. *Magn. Reson. Chem.* **2011**, *49*, 350−357.
(11) Martin, G. E.; Sunseri, D. *J. Pharm. Biomed. Anal.* **2011**, *55*, 895−901.
(12) Martin, G. E.; Hilton, B. D.; Willcott, M. R. III; Blinov, K. A. *Magn. Reson. Chem.* **2011**, *49*, 641−646.
(13) (a) Martin, G. E. In *Annual Reports in NMR Spectroscopy*; Webb, G. A., Ed.; Academic Press: New York, 2002; Vol. *46*, Chapter 2, pp 37−100. (b) Schoefberger, W.; Schlangnitweit, J.; Müller, N. In *Annual Reports in NMR Spectroscopy*; Webb, G. A., Ed.; Academic Press,: New York, 2011; Vol. *70*, Chapter 1, pp 1−60. (c) Furrer, J. In *Annual Reports in NMR Spectroscopy*; Webb, G. A., Ed.; Academic Press: New York, 2011; Vol. *74*, Chapter 6, pp 293−355.
(14) Krishnamurthy, V. V.; Russell, D. J.; Hadden, C. E.; Martin, G. E. *J. Magn. Reson.* **2000**, *140*, 232−239.
(15) Nyberg, N. T.; Duus, J. O.; Sørensen, O. W. *J. Am. Chem. Soc.* **2005**, *127*, 6154−6155.
(16) Nyberg, N. T.; Duus, J. O.; Sørensen, O. W. *Magn. Reson. Chem.* **2005**, *43*, 971−974.
(17) Benie, A. J.; Sørensen, O. W. *J. Magn. Reson.* **2007**, *184*, 315−321.
(18) Martin, G. In *Annual Reports in NMR Spectroscopy*; Webb, G. A., Ed.; Academic Press: New York, 2011; Chapter 5, pp 215−291.
(19) Bax, A.; Freeman, R.; Frenkiel, T. A. *J. Am. Chem. Soc.* **1981**, *103*, 2102−2104.
(20) Turner, D. L. *J. Magn. Reson.* **1983**, *49*, 175−178.
(21) Bax, A.; Mareci, T. H. *J. Magn. Reson.* **1983**, *53*, 360−363.
(22) Snyder, D. A.; Brüschweiler, R. In *Multidimensional NMR Methods in the Solution State*; Morris, G. A.; Emsley, J. W., Eds.; John Wiley and Sons, Ltd.: Chichester, 2010; Chapter 7, pp 97−105.
(23) In the covariance calculations described in this report, the F_1 dimension is the indirectly detected frequency domain and is oriented

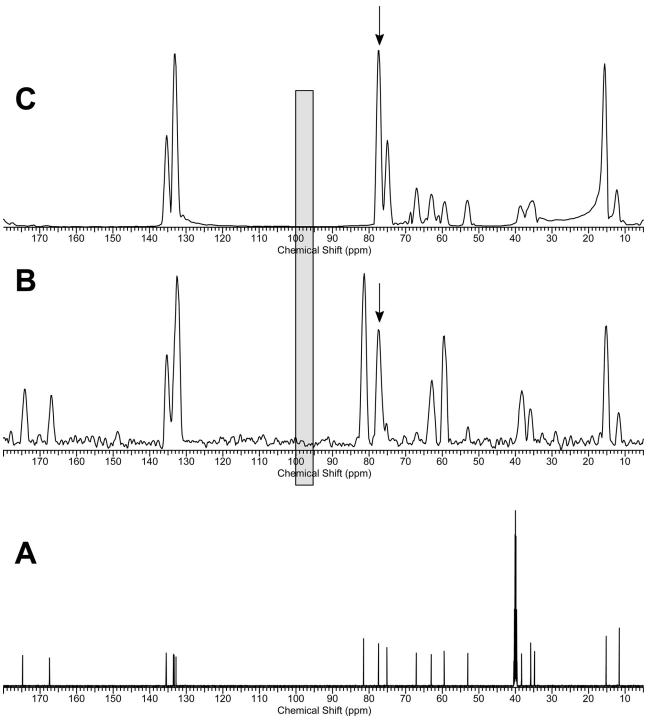

Figure 9. (A) ^{13}C reference spectrum of retrorsine (**1**) in DMSO-d_6. (B) F_1 projection of the 7 Hz optimized 1,*n*-ADEQUATE spectrum of retrorsine (**1**) recorded in 18 h 30 min. (C) F_1 positive projection of the 7 Hz optimized HSQC-1,*n*-ADEQUATE spectrum calculated from the spectrum shown in Figure 6 and a multiplicity-edited GHSQC spectrum using the GIC method (power = 0.5). Note that the projection of the 1,*n*-ADEQUATE spectrum shown in panel B contains the carbonyl resonances, whereas the F_1 projection of the HSQC-1,*n*-ADEQUATE spectrum shown in panel C does not. The carbonyl resonances are, instead, observed in the F_2 dimension of the HSQC-1,*n*-ADEQUATE spectrum at the F_1 shift of the carbon to which they are long-range coupled via $^nJ_{CC}$. The S/N ratio of the two spectra was determined using the region from 95 to 100 ppm (grayed box) as noise. The S/N ratio of the 1,*n*-ADEQUATE spectrum, using the C-5a resonance at 77.1 ppm (designated by the arrow), was 29:1. In contrast, the S/N for the corresponding resonance in the HSQC-1,*n*-ADEQUATE spectrum was 461:1, which is 16-fold greater.[10]

vertically ; the F_2 dimension is the directly detected frequency domain and is oriented horizontally. Our convention has been that the F_2 axis is derived from the high-sensitivity experiment, for example, the multiplicity-edited GHSQC spectrum, and that the F_1 axis is derived from the low-sensitivity, 1,1-ADEQUATE or 1,*n*-ADEQUATE experiment. In an HSQC-1,1- or -1,*n*-ADEQUATE spectrum, the indirectly detected nucleus occupies both dimensions; we label F_1 in the vertical dimension and F_2 in the horizontal dimension, admittedly a somewhat arbitrary choice. Correlations between protonated adjacent carbons are diagonally symmetric. Correlations between nonprotonated and protonated carbons are diagonally asymmetric; using the convention described here, the F_2 chemical shift cited would refer to the nonprotonated carbon and is detected at the F_1 chemical shift of the protonated carbon.

(24) Cheatham, S.; Kline, K.; Sasaki, R. R.; Blinov, K.; Elyashberg, M. E.; Molodtsov, S. G. *Magn. Reson. Chem.* **2010**, *48*, 571−574.

(25) Williamson, R. T.; Marquez, B. L.; Gerwick, W. H.; Koehn, F. E. *Magn. Reson. Chem.* **2001**, *39*, 544−548.

(26) Blinov, K. A.; Larin, N. I.; Williams, A. J.; Mills, K. A.; Martin, G. E. *J. Heterocycl. Chem.* **2006**, *43*, 163−166.

(27) Martin, G. E.; Hilton, B. D.; Irish, P. A.; Blinov, K. A.; Williams, A. J. *J. Nat. Prod.* **2007**, *70*, 1393−1396.

(28) (a) Marshall, J. M.; Miller, D. E.; Conn, S. A.; Seiwell, R.; Ihrig, A. M. *Acc. Chem. Res.* **1974**, *7*, 333−339. (b) Hansen, P. E. *Magn. Reson. Chem.* **1978**, *11*, 215−233. (c) Wray, V. *Prog. NMR Spectrosc.* **1979**, *13*, 177−256. (d) Marshall, J. L. *Carbon-Carbon and Carbon-Proton NMR Couplings: Application to Organic Stereochemistry and Conformational Analysis*; Verlag Chemie: Deerfield Beach, FL, 1983. (e) Komieiska-Trela, K. In *Annual Reports in NMR Spectroscopy*; Webb, G. A., Ed.; Academic Press: New York, 1995; Vol. *30*, Chapter 4, pp 131−230. (f) Krivden, L. B.; Della, E. W. *Prog. NMR Spectrosc.* **1991**, *23*, 301−610.